Characterizing Flocculated Suspensions with an Ultrasonic Velocity Profiler in Backscatter Mode

Serish Tanya Hussain
School of Chemical and Process Engineering, University of Leeds
Leeds, UK
pm14sth@leeds.ac.uk

Jeffrey Peakall
School of Earth and Environment, University of Leeds
Leeds, UK
J.Peakall@leeds.ac.uk

Martyn Barnes
Sellafield Ltd
Hinton House,
Warrington,UK
martyn.g.barnes@sellafieldsites.com

Timothy N. Hunter
School of Chemical and Process Engineering, University of Leeds
Leeds, UK
T.N.Hunter@leeds.ac.uk

***Abstract*— This paper reports on use of a commercial ultrasonic velocity profiler (UVP) to monitor changes in concentration within complex suspensions. A calcium carbonate ($CaCO_3$) nuclear waste simulant was used with a high molecular weight anionic polymer flocculant to produce varying suspension environments. 2 MHz ultrasonic transducers were used in both *in situ* and 'remote' configurations to extract backscatter voltage profiles of the suspensions, where the remote probes highlighted the ability of the UVP to analyze through pipe walls. Calibration was achieved by measuring logarithmic function of the backscatter voltage (*G*-function). Here, profile gradients averaged over selected distances and concentrations are used to measure particle attenuation coefficients. Both *in situ* and remote probes gave comparable results, where addition of polymer flocculant led to a decrease in the relative attenuation, due to lower viscous absorption with particle aggregates. Flocculated aggregates largely followed estimation from spherical scattering theory if aggregate density is taken account of. Attenuation constants can be used to determine single and dual inversions to measure concentration profiles in nuclear wastes.**

Keywords—UVP, Attenuation coefficients, Calcium carbonate, Flocculation, Nuclear waste

I. INTRODUCTION

This project focuses on the ability of acoustics to analyze and characterize nuclear waste suspensions. There are many types of complex nuclear waste deposits worldwide, such as at Sellafield (the UK's largest nuclear site), where wastes are in the form of complex precipitated sludge [1]. Chemical composition changes over time have led to uncertainties on the nature of these wastes, and to better understand their particulate properties, an *in situ* characterization technique is required [2]. Sellafield Ltd plan to transport these sludges in engineered pipelines to waste treatment plants or long-term storage facilities following characterization. The complex suspensions are expected to change through shear degradation via transport, which leads to breakdown of aggregates and decreasing particulate size [3]. Therefore, in this paper, nuclear waste simulant material has been analyzed *in situ* via a non-contact method. In particular, a remote acoustic system has been used to analyze calcium carbonate ($CaCO_3$). $CaCO_3$ is non-hazardous test material with a similar structure to common fine sludges [4]. It has also been extensively utilized as an analogue for nuclear wastes in experiments [5], which limits the risk of working with active sediment in non-controlled environments [6].

Acoustic backscatter systems (ABS) analyze sediment concentration by measuring scattering-attenuation properties [7]. Attenuation is dependent on a range of factors including, but not restricted to, sediment type, concentration, and size [8]. In a previous study, the current authors investigated the effect of concentration on sound attenuation through homogeneous suspensions of glass beads [7]. For a more industrially relevant system, this work considers aggregated and flocculated $CaCO_3$ suspensions, using high molecular weight anionic polymers [9]. Addition of flocculant changes the suspension d_{50} to more than seven times its original value (from ~7 μm to 54 μm) [5] allowing analysis of suspensions with different size distributions. The specific ABS used is a commercial ultrasonic velocity profiler (UVP) [10]. The UVP is utilized to analyze the suspension velocity through Doppler shift, however here, it has been used to extract acoustic backscatter amplitude profiles [11]. The UVP has a frequency range from 0.5 to 8 MHz, where multiple transducers of same frequency can be used, or several transducers of varying frequency. Transducers compatible with this UVP have active radii of 2.5 or 5 mm. For flow monitoring applications, only 2.5 mm were deemed suitable [12]. Suspensions of $CaCO_3$ with and without high molecular weight flocculant are analyzed with a UVP at various concentrations, where backscatter profiles are extracted [13]. An established calibration tank is employed to ensure homogeneous concentrations [7]. Probes inserted *in situ*, and in a 'remote' configuration (on the tank exterior) are used to investigate applicability of analysis through tank or pipe walls. Attenuation constants are extracted by establishing the '*G*-function', which is a log voltage function dependent on distance [13]. The *G*-function allows characterization of overall suspension attenuation behavior, where role of particle aggregation on ultrasonic scattering is highlighted. Comparison is made through the dimensionless χ-function.

Sellafield Ltd

II. Theory

The UVP outputs data in raw echo amplitude form ($E(r)$ in Volts) which must be converted to voltage $V(r)$ (1). Conversion is dependent on a user identified gain function ($g(r)$) which ranges from 1-9. For experiments presented, an intermediate value of 6 was used to ensure accurate data amplification [7]. Calculated voltage is used to determine a logarithmic voltage function known as 'G' (in ln (V.m)) see (2), where r (m) is the distance from the transducer. A nearfield correction factor (ψ) is required for conversion; however, it is assumed to be unity outside the nearfield region (0.025 m) [14][15]. The G-function is also a function of concentration (M, in g/L), attenuation due to solid (α_s, in m^{-1}) and water (α_w, in m^{-1}) as well as the transducer constant (k_t, in $V.m^{1.5}$) and backscatter coefficient (k_s, in $m.kg^{0.5}$) [7].

$$V(r) = [3.052 \times 10^{-4} E(r)] / g(r) \quad (1)$$

$$G = \ln(\psi r V) = \ln(k_s k_t) + 0.5\ln(M) - 2r(\alpha_w + \alpha_s) \quad (2)$$

The normalized scattering cross-section (χ) is calculated using the heuristic expression from Betteridge *et al.* [16], which is a function of angular wavenumber (k, in m^{-1}) and particle radius (a, in m). This expression is an approximation for spherical glass particles [7].

$$\chi = [0.24(1 - 0.4\exp[(5.5-ka)/2.5^2])(ka)^4]/ [0.7 + 0.3(ka) + 2.1(ka)^2 - 0.7(ka)^3 + 0.3(ka)^4] \quad (3)$$

For calibration, the concentration independent attenuation constant (ξ, in $m^2.kg^{-1}$), where $\xi = \alpha_s/M$, is extracted by taking a double differentiation of the G-function versus concentration [7] (4). Experimental constants are used to calculate χ using particulate density (ρ_s, in $kg.m^{-3}$) and radius (a, in m) as in (5).

$$\xi = -0.5(\partial^2 G/\partial M \partial r) = -0.5\,(\partial/\partial M)\,[(\partial/\partial r)\ln(\psi r V)] \quad (4)$$

$$\chi = [\xi\,(4a \times \rho_s)] / 3 \quad (5)$$

III. Experimental Methods

A. Materials

Calcite (Omyacarb 2, Omya AG) a crystal form of calcium carbonate, was used for all experiments. Water-soluble anionic polyacrylamide-poly(acrylic acid) copolymer, AN934SH (SNF Ltd) was used, with a molecular weight of roughly 1.4×10^6 $g.mol^{-1}$ [9]. 1000 ppm stock aqueous solution was prepared by adding 1 g of polymer into a 1 L vessel, at a rate of 0.1 g/min. A mixer (at 400 rpm) was used to distribute polymer in the vessel and left overnight to ensure it had fully dissolved. Particle diameter (d_{50} = 7μm) for non-flocculated calcite was found using a Mastersizer 3000 (Malvern-Panalytical Ltd).

B. Methods

Initially, un-flocculated $CaCO_3$ was suspended in a conical based Perspex calibration tank (10 mm thick) at a concentration of 27.5 g/L. The tank contained a mixer impeller system to ensure the suspension remained homogeneous (operating at 350 rpm) and a pump recirculation loop (at 75 rpm) to redistribute any settled material. A schematic of the experimental set-up is shown in Fig.1. The tank was emptied halfway and diluted with water to produce a 13.5 g/L suspension, where this process was repeated until the suspension concentration was 3.38 g/L. For the flocculated experiments, the 1000 ppm stock flocculant solution was added to the 27.5 g/L $CaCO_3$ suspension dropwise over 4 min, for a bulk polymer concentration of 20 ppm (consistent with previous reported levels for efficient flocculation with this polymer [5],[9]). The same dilution procedure was repeated for the flocculated suspensions with the equipment kept in the same position through both experiments. For flocculated suspensions, the particle diameter was determined using an *in situ* focused beam reflectance meter (FBRM) (Mettler Toledo) giving a $d_{50\text{-}floc}$ = 54 μm. The FBRM was run in tandem with the acoustic experiments, where no significant change in the median size was evident over time.

For acoustic experiments, a UVP-DUO (Met-flow) commercial ultrasonic velocity profiler was used. At each concentration stage, a 2.5 mm radii 2 MHz transducer was placed vertically within the tank to extract *in situ* data, and another 'remote' probe placed horizontally outside the tank, held flush to ensure good penetration [12], and above the mixer to reduce disturbance (see Fig. 1). This system allowed direct measurements from non-contact probes, which can be mounted on pipes to monitor profiles in flow. Both transducers ran simultaneously to ensure the suspension environment was constant. A time delay of 100 ms echo disturbance was set between transducers. The measurement time for each transducer was 60 ms pulse for each with a 100 ms delay between transducers, for the two transducers, this is a 220 ms per profile total time. For all 1023 profiles, this is a total time of 225 seconds [12].

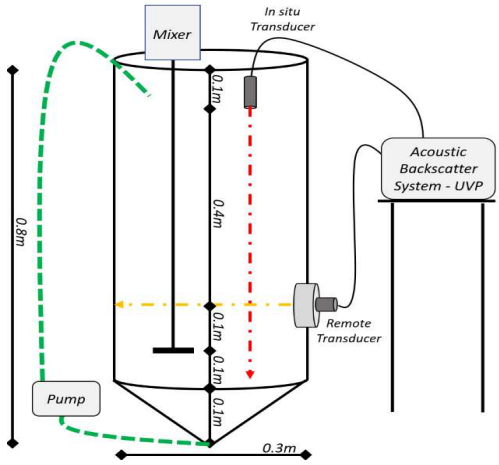

Fig. 1. Schematic of the calibration tank and UVP probe arrangement.

IV. Results and Discussion

Acoustic G-function profiles collected from the *in situ* probe are shown in Fig. 2, for two concentrations. Orange/red profiles indicate flocculated $CaCO_3$ data and light-blue profiles shows data from un-flocculated $CaCO_3$. Peak decay in all profiles within the first 0.04 m infer a complex nearfield environment [15]. Therefore, this region is ignored, and all data was extracted from 0.04 to 0.12 m. Average gradient (dG/dr) values for each system in this region are shown by dashed black lines, and as described in Section II, were used to calculate attenuation coefficients. The secondary increase in G at larger distances after 0.12 m are indicative of mathematical artifacts, from hitting the

system noise floor [17]. This trend is shown for both 27.5 g/L profiles, where it suggests the noise floor is reached at a *G*-function value of approximately -6.8, highlighting the UVP limit for sound profiling.

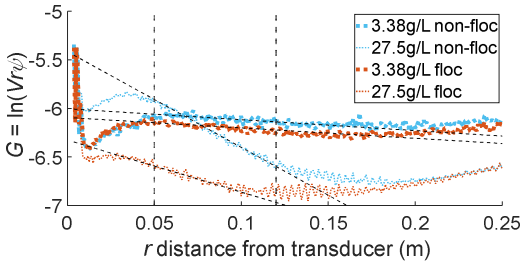

Fig. 2. Acoustic *G*-function profiles extracted using *in situ* transducers.

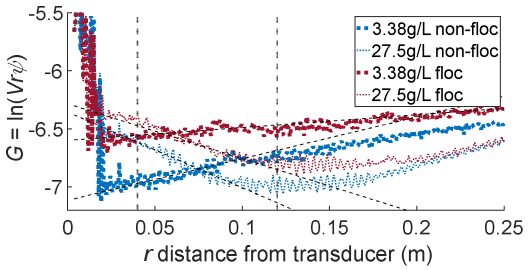

Fig. 3. Acoustic *G*-function profiles extracted using 'remote' transducers.

At 3.38 g/L, acoustic profiles of flocculated $CaCO_3$ and non-flocculated $CaCO_3$ show slight differences in attenuation (as measured from the gradient). The higher concentration of 27.5 g/L allows the user to observe clearer deviations between flocculated and non-flocculated environments. The non-flocculated profile in Fig. 2 shows a much steeper gradient in *G* versus *r*, inferring a higher level of overall attenuation for non-flocculated suspensions. Such differences were initially considered counter intuitive, as it is expected that the greater particulate size of flocculated systems would enhance attenuation through greater non-directional particle scattering. In this case though, the non-flocculated systems are small enough in size to cause a considerable increase in viscous absorption effects that increases overall attenuation. Similar enhanced viscous attenuation has previously been evidenced in other fine mineral nuclear waste analogues [18]. Fig. 3 presents the same acoustic *G*-function profiles extracted using remote transducers. The respective relationship between flocculated and non-flocculated systems are similar, as for the *in situ* probes in Fig. 2, with flocculated systems showing lower levels of attenuation (lower gradient of *G*). Interestingly, for lower concentrations, *G*-function gradients were positive across the distance range, suggesting a larger reflection of sound at greater distances with lower concentration of particles. Such behavior would be considered un-physical, but similar positive gradients in *G*-function have been found in various systems at low concentrations, when incorrect nearfield correction factors have been used [5]. It appears impedance and signal disruption through the tank wall cause additional nearfield interference than evidenced with *in situ* probes. It was evident that average signal strength for remote probes was weaker (lower average *G*-values) due to signal loss with propagation through tank walls [19].

The gradients for all profiles over the operational distance sections in Figs. 2 and 3 (d*G*/d*r*) – shown by the dashed black lines – are plotted against the corresponding concentration to produce an attenuation profile, as presented in Fig. 4. This is given for the two environments (non-flocculating and flocculating) using both *in situ* and remote ultrasonic transducers. The concentration independent attenuation coefficients (ξ) are extracted by taking half of the negative gradient value for each system (see (4)). The non-flocculated suspensions both exhibit a steeper attenuation gradient, indicative of the greater loss of sound across the suspension, due to the viscous attenuation as described. Interestingly, while the values of *G* are smaller for the remote probes for all concentrations (due to signal loss through the tank wall, as discussed) the actual overall gradient values of d*G*/d*r* for all systems are within 10% of the *in situ* profiles. This result provides evidence that the remote transducers can accurately analyze the acoustic properties, highlighting the applicability of non-contacting probe arrangements for on site applications.

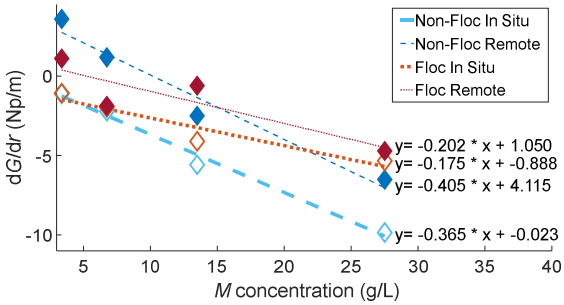

Fig. 4. Change in d*G*/d*r* (Np/m) with concentration for non-flocculated and flocculated dispersions, using either *in situ* or 'remote' probes.

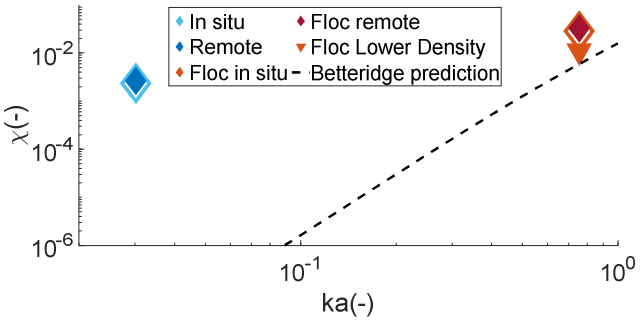

Fig. 5. Normalized scattering cross-section against wavenumber and particle radius for non-flocculated (blue) and flocculated (orange/red) environments using *in situ* (filled) and remote (non-filled) transducers. Also shown is the spherical scattering prediction by Betteridge *et al.* [16].

In Fig. 5, normalized scattering cross section (χ) was calculated for all datasets, using measured attenuation coefficients. The heuristic expression from Betteridge *et al.* [16] for spherical glass particles is plotted for comparison. It is noted that to calculate χ, the mean particle radius for non-flocculated species determined from the Mastersizer (a = 3.5 µm) was used, while for the flocculated species, the mean particle radius from the FBRM (a = 27 µm) was used. Initially, the particle density of calcite $CaCO_3$ (ρ_s = 2710 kg/m^3) was used in the calculation (5). Consistent with similar attenuation values evidenced in Fig. 4, χ values calculated from remote probes are almost identical to the *in situ* data, for flocculated and non-flocculated systems. It is evident that non-flocculated values are considerably greater than predicted by the theoretical Betteridge expression. Overprediction is due to the expression only considering attenuation from particle scattering (assumed to be minimal

for fine particles). It does not include attenuation from viscous adsorption, and current work is looking to incorporate these effects, using Urick's model [18].

Flocculated data (in orange/red) compares more closely to the Betteridge estimation, although χ values are still underpredicted. One potential reason is that as flocculated aggregates contain significant bound water between particles, the use of particle density is likely not correct. Therefore, a further calculation was made to estimate flocculated χ value, using a lower density value ($\rho_{s\text{-}lower}$ = 1045 kg.m^{-3}) denoted by the inverse orange triangle. This lower density estimate was based on values for similar flocculated magnesium hydroxide [9] and provides a low limit for χ, highlighting the difficulty in accurately deriving values. As most of the suspension is water, bulk density is expected to be closer to the lower flocculant density limit. Despite uncertainties, it is clear that using a lower floc density results in closer correlation to Betteridge spherical scattering theory, suggesting additional scattering-attenuation contributions of aggregates are low, as long as the overall density is taken account of. It is lastly noted also that the FBRM natively measures chord length distribution, rather than particle size directly. Particle radius values (a) can be variable from the FBRM, depending on whether number or square weighted distributions are extracted. Values reported here are based on number weighted, as they provide reliable values when comparing to manufacturer listed particle radius for non-flocculated dispersions. However, square weighted distributions will shift values higher on the ka axis, which may modify flocculated χ values relative to predictions. Again, this uncertainty shows how complicated it is to analyze flocculated suspensions.

V. CONCLUSIONS

- Here, a UVP in backscatter mode, was used to characterize flocculated and non-flocculated nuclear waste simulant suspensions. Probes in a calibration tank were positioned *in situ* and in a non-contacting 'remote' arrangement, for future monitoring applications.
- *In situ* and remote probes gave comparable suspension attenuation coefficients for all systems. Remote probes had a lower signal-to-noise ratio, due to loss through tank walls. The noise floor for the UVP, using the *G*-function, was found to be approx. -6.8 for all profiles.
- Flocculated suspensions (larger particle size) attenuated less and exhibited a predictable scattering cross section, if the reduced overall aggregate density is taken account of. Un-flocculated particulate suspensions had greater attenuation and overall scattering cross section, where the increased attenuation was due to viscous losses.
- Analyzing flocculated suspensions is difficult, due to variation of density and particle radius, but the quality of data in this paper has been found to be accurate.

ACKNOWLEDGMENTS

The authors thank the Engineering and Physical Sciences Research Council (EPSRC) UK and Sellafield Ltd for funding through the Next Generation Nuclear (NGN) Centre for Doctoral Training (EP/L015390/1).

REFERENCES

[1] Jackson, S.F., Monk, S.D. and Riaz, Z. An investigation towards real time dose rate monitoring, and fuel rod detection in a First-Generation Magnox Storage Pond (FGMSP). *Applied Radiation and Isotopes.* 2014, **94**(1), pp.254-259.

[2] Gregson, C.R., Goddard, D.T., Sarsfield, M.J. and Taylor, R.J. Combined electron microscopy and vibrational spectroscopy study of corroded Magnox sludge from a legacy spent nuclear fuel storage pond. *Journal of Nuclear Materials.* 2011, **412**(1), pp.145-156.

[3] Adams, J.F.W., Biggs, S.R., Fairweather, M., Yao, J. and Young, J. Transport of Nuclear Waste Flows: A Modelling and Simulation Approach. In: *ASME 14th Conference on Environmental Remediation and Radioactive Waste Management, January 2011, France.* France: ASME, 2011, pp. 267-275.

[4] Omya North America. AZ Calcium Carbonate. *Omya.* [Online]. 2021. [Accessed 16 April 2021]. Available from: Omya OMYACARB® 2 - AZ Calcium Carbonate (matweb.com)

[5] Hunter, T.N. et al. Concentration profiling of a horizontal sedimentation tank utilizing a bespoke acoustic backscatter array and CFD simulations. *Chemical Engineering Science.* 2020. **218**, 115560.

[6] Paul, N., Biggs, S., Edmundson, M., Hunter, T.N. and Hammond, R.B. Characterizing highly active nuclear waste simulants. *Chemical Engineering Research and Design.* 2013, **91**(4), pp.742-751.

[7] Hussain, S.T., Hunter, T.N., Peakall, J. and Barnes, M. Utilization of underwater acoustic backscatter systems to characterize nuclear waste suspensions remotely. *Proceedings of Meetings on Acoustics*. 2020, **40**, 070005; doi: 10.1121/2.0001303.

[8] Sassi, M.G., Hoitink, A.J.F. and Vermeulen, B. Impact of sound attenuation by suspended sediment on ADCP backscatter calibrations. *Water Resources Research.* 2012, **48**(9), pp. 1-14.

[9] Lockwood, A.P.G., Peakall, J., Warren, N.J., Randall, G., Barnes, Martyn., Harbottle, D. and Hunter, T.N. Structure, and sedimentation characterization of sheared $Mg(OH)_2$ suspensions flocculated with anionic polymers. *Chemical Engineering Science.* 2021, **231**, 116274.

[10] Chakraborty, B., Mahale, V., Navelkar, G., Rao, B.R., Prabhudesai, R.G., Ingole, B. and Janakiraman, G. Acoustic characterization of seafloor habitats on the western continental shelf of India. *ICES Journal of Marine Science.* 2007, **64**(3), pp. 551-558.

[11] Takeda. Y. ed. Ultrasonic Doppler Velocity Profiler for Fluid Flow. New York: Springer Publishing, 2012.

[12] MET-FLOW. *Products/ Profilers*. [Online]. 2021. [Accessed 16 April 2021]. Available at: https://met-flow.com/technology/products/uvp-duo-profilers/

[13] Rice, H.P., Fairweather, M., Peakall, J., Hunter, T.N., Mahmoud, B. and Biggs, S.R. Measurement of particle concentration in horizontal, multiphase pipe flow using acoustic methods: Limiting concentration and the effect of attenuation. *Chemical Engineering Science*. 2015, **126**(1), pp. 745-758.

[14] Downing, A., Thorne, P. D. & Vincent, C. E. Backscattering from a suspension in the near field of a piston transducer. *Journal of the Acoustical Society of America*. 1995, **97**(3), pp. 1614-1620.

[15] Rice, H. P. Transport, and deposition behavior of model slurries in closed pipe flow Intellectual property and publication statements. Ph.D. thesis, University of Leeds, 2013.

[16] Betteridge, K. F., Thorne, P. D. & Cooke, R. D. Calibrating multi-frequency acoustic backscatter systems for studying near-bed suspended sediment transport processes. *Continental Shelf Research*. 2008, **28**(2), pp. 227-235.

[17] Kutluay, S., Ceyhand, A.A., Sahin, O. and Izgi, M.S. Utilization of In Situ FBRM and PVM Probes to Analyze the Influences of Monopropylene Glycol and Oleic Acid as Novel Additives on the Properties of Boric Acid Crystals. *Ind. Eng. Chem. Res.* 2020, **59**(19), pp. 9198-9206.

[18] Bishof, M., Zhang, X., Martin, M. and Ye, J. Optical Spectrum Analyzer with Quantum-Limited Noise Floor. *Physical Review Letters.* 2013, **111**(9) 093604.

[19] Urick, R.J. The Absorption of Sound in Suspensions of Irregular Particles. *The Journal of the ASA.* 1948, **20**(283).

[20] Prek M. Experimental Determination of the Speed of Sound in Viscoelastic Pipes. *International Journal of Acoustics and Vibration*. 2000, **5**(3), pp.146-150.